Study of Neoclassical Core Transport of Intrinsic Impurities in the National Spherical Torus Experiment

F. Scotti[1], V.A. Soukhanovskii[2], R.E. Bell[1], W. Guttenfelder[1], S. Kaye[1],
S. Gerhardt[1], R. Kaita[1], B.P. Leblanc[1] and the NSTX Team
[1] *PPPL, Princeton, NJ (USA)*
[2] *LLNL, Livermore, CA (USA)*

INTRODUCTION - Wall conditioning via lithium evaporative coatings led to the achievement of high confinement ELM(edge localized mode)-free H-mode regimes in the National Spherical Torus Experiment (NSTX)[1] and the consequent possibility of studying impurity sources, transport, and particle balances without the complications associated with ELMs. In NSTX, the main intrinsic impurities are carbon and lithium. Even though the graphite plasma facing components (PFCs) are covered with lithium coatings, significant carbon sputtering is still observed due to degradation of the thin lithium coatings at the strike point location as it is evident from post-run analysis of lithium coverage of divertor graphite tiles [2] and spectroscopic analysis of divertor carbon influxes [3]. While all the processes of carbon and lithium transport that lead sputtered impurities to the confined plasma need to be taken into consideration, including parallel and perpendicular SOL transport, this paper concentrates on the differences in impurity core transport regimes. Typically, both neoclassical and anomalous transport need to be taken into account in tokamaks to explain core impurity behavior, however, spherical tori have shown impurity transport close to the neoclassical levels both in CDX-U [4] and in NSTX [5] H-mode discharges. In this paper, the discussion will be limited to the differences in neoclassical transport regimes between the main intrinsic impurities and their relevance to experimentally observed trends. A more detailed analysis of the consistency of neoclassical transport with experimental levels of particle impurity transport in NSTX will be the subject of upcoming work.

EXPERIMENT - The analysis is based on high triangularity, high elongation ($\delta \sim 0.7$, $\kappa \sim 2.2$), H-mode, ELM-free, NBI heated (4 MW) discharges with lithium conditioning (170 mg applied on the lower divertor PFCs). Impurity densities (C and Li) in the core are measured by charge exchange recombination spectroscopy (CHERS) [8]. Carbon densities (n_C) are obtained from the C VI, $n = 8-7$ transition at 529.1 nm while lithium densities (n_{Li}) are inferred from the Li III, $n = 7-5$ transition at 516.7 nm, measured using the same CHERS system after replacing the transmission gratings. It must be noted that due to the contamination of the Li III charge exchange line with a C VI line ($n = 14-10$), n_{Li} must be understood as an upper estimate of the core n_{Li}, typically by a factor of the order of 2 [9]. A low concentration ($\leq\sim 1\%$) peaked n_C profile in L-mode typically evolves into a strongly hollow n_C profile at the H-mode transition with a steady slower accumulation into the core and concentrations up to $\sim 10\%$. Lithium ions show a similar profile evolution but with the extremely low core n_{Li} of $\sim 1\%$ of core n_C. Furthermore, as it can be seen in Figure 1, the ratio of the core lithium inventory over the core carbon inventory decreases during the discharge. As it is evident from Figure 1, carbon profiles do not reach steady state during the $\sim 1s$ NSTX discharges, with carbon accumulation causing dilution of the deuterons and lack of particle control (up to 50% of the total electron inventory due to carbon by end of discharge).

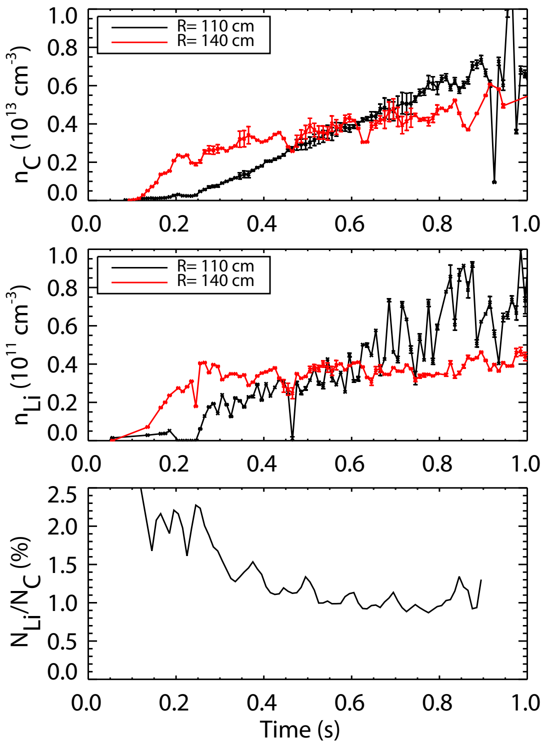

Figure 1: Carbon (top) and lithium (middle) densities in core and edge plasma as obtained from CHERS diagnostic for a lithium conditioned discharge. The ratio of the lithium to carbon inventory is plotted in the bottom plot (130725-130727).

In a typical ELM-free H-mode NSTX discharge, deuterium ions are well inside the banana-plateau regime while both carbon and lithium ions are in plateau regime in the core and in Pfirsch-Schlüter regime for r/a larger than respectively 0.4 and 0.6. Carbon is a strong impurity (impurity strength $\alpha_C = \frac{n_C Z_C^2}{n_D} \geq 5$ at $r/a \sim 0.8$) mostly collisional on deuterium ions ($\nu_{CD} \sim 10^4 s^{-1}$, $\nu_{CLi} \sim 5 \times 10^2 s^{-1}$) while lithium is a weak impurity ($\alpha_{Li} \sim 0.02$ at $r/a \sim 0.8$), mostly collisional on background carbon ions ($\nu_{LiD} \sim 5 \times 10^3 s^{-1}, \nu_{LiC} \geq \sim 5 \times 10^4 s^{-1}$), thus the importance of including multi-ion effects for lithium transport [10, 11]. For carbon, ambipolarity in the radial fluxes is satisfied to zeroth order in $\sqrt{m_e/m_D}$ with deuterium fluxes ($Z_C \Gamma_{r-C} = -\Gamma_{r-D}$) [11].

MODELING AND RESULTS - In this work, the neoclassical transport codes NCLASS [6] and NEO [7] were used in order to derive neoclassical fluxes and transport coefficients in mixed regimes, multi impurity NSTX plasmas (two impurity species were included C^{6+} and Li^{3+} with densities obtained from CHERS measurements). NEO was run using the full linearized Fokker-Plank collisional operator [12] and with the inclusion of toroidal rotation effects on equilibrium densities and radial fluxes [13]. In particular, neoclassical radial impurity particle fluxes can be written as a combination of a diffusive and a convective component.

$$\Gamma_r^{NC} = -D_r^{NC} \nabla n_Z + v_r^{NC} n_Z, \tag{1}$$

where Γ_r^{NC} is the radial particle flux, D_r^{NC} is the diffusion coefficient and v_r^{NC} is the convective velocity.

The very low lithium concentrations allowed a sensitivity study on n_{Li} with minor perturbation to the overall n_e profiles. n_{Li} was then varied in subsequent NCLASS runs (adjusting n_e to satisfy quasineutrality) between 0.01 and 100 times the experimental n_{Li}. NCLASS indicates a negligible effect on carbon transport due to the presence of lithium ions as was also suggested from collisionality estimates. Effects on the neoclassical carbon fluxes and transport coefficients can be seen only at $n_{Li} \sim 100$ times the experimental n_{Li}. At these values of n_{Li}, carbon would become predominantly collisional on lithium ions. The presence of background lithium ions is not responsible for the increased carbon ion confinement observed in lithium conditioned discharges, and carbon transport is mostly driven by main ions. Consider then only the Pfirsch-Schlüter component of carbon transport due to friction on main ions [11]:

$$\Gamma^C_{PS} = \frac{q^2 n_D \rho_D^2 \nu_{DC}}{Z_C} \times \left[K \left(\frac{\partial ln n_D}{\partial r} - \frac{Z_D}{Z_C} \frac{\partial ln n_C}{\partial r} \right) + H \frac{\partial ln T_D}{\partial r} \right]. \quad (2)$$

In plasma conditions (main ion collisionality and impurity strength) typical of NSTX H-mode plasmas, K is equal to its asymptotic value 1 and H is equal to its asymptotic value -0.5. The deuterium ∇T_D term always provides a screening term (given a monotonically decreasing T_D profile), while a monotonically decreasing deuteron density (n_D) profile would lead to an inward term in the impurity flux. In lithium conditioned H-mode discharges, the edge ∇T_D is reduced and neoclassical carbon transport is then mostly driven by the ∇n_D term.

Lithium transport, on the other hand, is mostly driven by collisions on carbon ions. The high background carbon density leads to an increase in lithium particle diffusivities (D_{Li}). In Figure 2, the diffusion coefficients and convective velocities are plotted for the two different impurities as computed using NCLASS and NEO. The transport coefficients are calculated from the impurity radial particle fluxes Γ_{r-z} via a scan in the impurity density gradient. Diffusivity and convective velocity are obtained respectively from the slope and the intercept of the linear fit of Γ_{r-z}/n_z versus $-\nabla n_z/n_z$ and are dependent on the flux surface label choice. One can immediately see the difference in transport coefficients for carbon and lithium ions with lithium showing an order of magnitude higher edge diffusivity with comparable or

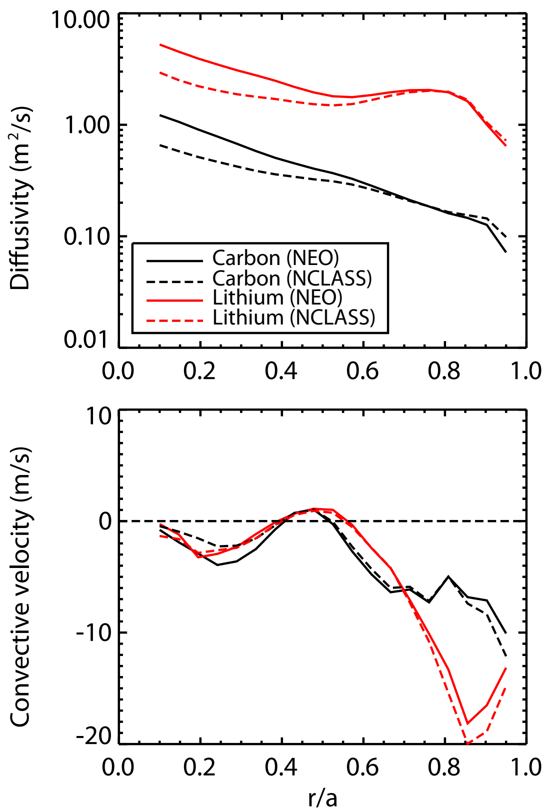

Figure 2: NEO and NCLASS diffusivity, convective velocity for carbon and lithium ions (130725, t=0.445s).

higher inward edge convective velocities. The outward directed lithium radial particle flux for $r/a \geq 0.8$ indicates that lithium edge fluxes are dominated by the diffusive component. NEO and NCLASS are in good agreement showing differences only inside of r/a=0.6 due to the effects of toroidal rotation that are neglected in NCLASS calculations. It must also be noted that the supersonic impurity flow can cause redistribution of the impurity density on a given flux surface. In this case, the redistribution, as calculated by NEO, was as much as 15-20% for n_C if compared to the flux surface average density.

The difference in the two impurities transport characteristics was modeled using the MIST code [14] in a predictive mode. Using the experimental T_e and n_e, the neoclassical transport coefficients for carbon and lithium calculated by NCLASS were used in order to model the time evolution of the charge state distribution of the two impurities given the same edge impurity source. Modeling with the MIST code shows how the high core D_{Li} results in core n_{Li} that varies from $\sim$ 10% to a few % of n_C, decreasing with the increase in n_C over time. This is qualitatively consistent with the low n_{Li} observed in the NSTX core as well as with the decrease of the lithium-to-carbon inventory as the discharge progresses. However, experimentally measured n_{Li} are usually 1% of n_C or less since the early phase of the discharge indicating the possible importance of high divertor retention of sputtered lithium, that would effectively reduce the lithium edge source [3]. A detailed comparison with experimental profiles shapes and evolution for both carbon and lithium is now ongoing and is needed in order to verify the consistency of neoclassical transport to the experimental levels.

Work supported by U.S. DOE Contract DE-AC02-09CH11466 and DE-AC52-07NA27344. The authors would like to acknowledge Dr. Robert Andre for useful discussions and assistance with NCLASS and Dr. Emily Belli and Dr. Jeff Candy for the availability of NEO code and useful discussions.

References

[1] M.G. Bell et al., Plasma Phys. Control. Fusion 51(12), 2009.
[2] W. Wampler et al., J. Nucl. Mater., 390-391, 1009, 2009.
[3] F. Scotti, submitted to J. Nucl. Mater., 2012.
[4] V. A. Soukhanovskii, et al., Plasma Phys. Contr. Fusion 44, 2339, 2002.
[5] L. Delgado-Aparicio, et al., Nucl. Fusion, 49(8):085028, 2009.
[6] W.A. Houlberg et al., Phys. Plasmas 4 (9), 1997.
[7] E.A. Belli et al., Plasma Phys. Control. Fusion, 50, 095010, 2008.
[8] R.E. Bell, et al., Rev. Sci. Instrum., 81, 10D724, 2010.
[9] M. Podesta, et al., Nucl. Fusion, 52, 033008, 2012.
[10] S.P. Hirshmann et al., Nucl. Fusion, 21, 1079, 1981.
[11] K. Wenzel et al., Nucl. Fusion, 30, 1117, 1990.
[12] E.A. Belli et al., Plasma Phys. Control. Fusion, 54, 015015, 2012.
[13] E.A. Belli et al., Plasma Phys. Control. Fusion, 51, 075018, 2009.
[14] R. Hulse, Nucl. Technol. Fusion 3 (259), 1983.